Research Update: Density functional theory investigation of the interactions of silver nanoclusters with guanine

Brandon B. Dale, , Ravithree D. Senanayake, and , and Christine M. Aikens

Citation: APL Materials **5**, 053102 (2017); doi: 10.1063/1.4977795
View online: http://dx.doi.org/10.1063/1.4977795
View Table of Contents: http://aip.scitation.org/toc/apm/5/5
Published by the American Institute of Physics

APL MATERIALS **5**, 053102 (2017)

Research Update: Density functional theory investigation of the interactions of silver nanoclusters with guanine

Brandon B. Dale, Ravithree D. Senanayake, and Christine M. Aikens
Department of Chemistry, Kansas State University, Manhattan, Kansas 66506, USA

(Received 15 December 2016; accepted 9 February 2017; published online 6 March 2017)

Bare and guanine-complexed silver clusters Ag_n^z (n = 2-6; z = 0-2) are examined using density functional theory to elucidate the geometries and binding motifs that are present experimentally. Whereas the neutral systems remain planar in this size range, a 2D-3D transition occurs at Ag_5^+ for the cationic system and at Ag_4^{2+} for the dicationic system. Neutral silver clusters can bind with nitrogen 3 or with the pi system of the base. However, positively charged clusters interact with nitrogen 7 and the neighboring carbonyl group. Thus, the cationic silver-DNA clusters present experimentally may preferentially interact at these sites. [http://dx.doi.org/10.1063/1.4977795]

I. INTRODUCTION

Over the years, gold and silver nanoparticles have demonstrated fascinating optical and chemical properties that depend on the size of the particle.[1–3] Small sized metal nanoclusters (with diameters up to around 2 nm) are considered to be brighter and more photostable fluorophores[4–11] compared to existing organic dyes as well as smaller and less toxic compared to quantum dots.[12] In particular, silver nanoclusters (AgNCs) are of interest, and these systems involve stabilizing ligands to prevent them from oxidation and aggregation.[13] Dendrimers, synthetic polymers, biopolymers, thiol ligands, and inorganic matrices have been used as the stabilizing ligands for AgNCs.[6,11,14–17] In 2004, Dickson and coworkers first discovered the formation of DNA-templated Ag nanoclusters (DNA-AgNCs) where they showed that DNA acts as a template for the time-dependent and size-specific formation of nanoclusters.[18] Since then, DNA-AgNCs have become a research field of growing interest.

Importantly, DNA stabilized Ag nanoclusters have attracted much attention due to the tunability of the emission characteristics with different DNA templates. It has been shown that the emission wavelength can be varied from violet to near infrared in DNA-AgNCs.[19–22] Therefore, DNA-AgNCs have been identified as potential candidates to be utilized in various applications such as bioimaging, biolabeling, catalytic reactions, and analyte and ligand sensing.[4–7,14,23–26] The emission tunability can also be altered through experimental conditions,[19,20,27,28] but changing the DNA template itself is considered superior due to the higher functionality in the DNA-AgNCs through emission tuning.[13]

Various research groups have conducted extensive experimental investigations on DNA-AgNCs. Many studies have been performed to understand the effects from the DNA base pairs on the small AgNCs ($\sim Ag_2$-Ag_{30})[18,29–32] and some provide insights into creating AgNCs using different DNA platforms.[4,5,8,10] Their findings indicate that it is possible to manipulate the size and formation of these nanomaterials by employing strands of DNA with specific sequences.[3,18,29,30,32] Dickson, Petty, and coworkers have shown that very small ($n < 10$) AgNCs can be synthesized by exploiting the DNA sequence.[30] Gwinn's group and Dickson's group have done studies especially on short single-stranded DNA.[8,9,33–36] Yeh, Martinez, Werner, and co-workers have carried out investigations on DNA detection probes with a greater focus on guanine bases.[12,23,37–39]

In addition to the experimental work, theoretical investigations have also been performed on DNA-AgNCs by several groups. Gwinn and coworkers have studied the binding of DNA bases (adenine, cytosine, guanine, and thymine) with neutral silver clusters Ag_n (n=1-6) and the absorption spectra of these complexes using density functional theory (DFT).[40] A DFT investigation was

performed by Lopez-Acevedo and coworkers to understand the DNA/RNA base interactions with gold and silver atoms with different charge states (neutral, cationic, and anionic).[41] In a combined experimental-theoretical study, Gwinn, Lopez-Acevedo, and coworkers have shown a higher stability in Ag^+-mediated pairing of guanine homo-base strands than canonical guanine-cytosine pairing.[42] Kononov's group has investigated the excitation and emission properties of several DNA-AgNCs using time dependent DFT and QM/MM calculations.[43,44] The structural sensitivity of the chiroptical activity of DNA-AgNCs has been studied by Gwinn, Aikens, and coworkers to suggest cluster structures.[45] Additional work focuses on the electronic and optical properties of DNA-AgNCs,[2,46] charge transfer optical absorption mechanisms,[47] and the photophysics of the excitation process involved in DNA-AgNCs.[48]

Despite the extensive experimental and theoretical work on the DNA-AgNC systems, the binding interaction of the Ag_n nanoclusters with the base pairs is still not fully understood. Further progress of DNA-AgNC nanomaterials is hindered by the limited understanding of the cluster structure. It is vital to understand the relationship between the structure and the DNA sequences that lead to different emission characteristics for the potential applications. In this study we investigate the interactions of small pure silver clusters (Ag_n, n = 2-6) in neutral, cationic, and dicationic forms with guanine in order to provide insights into the structures that are potentially present in these systems.

II. COMPUTATIONAL METHODS

In this work, the Amsterdam Density Functional (ADF)[49,50] package was utilized. The Becke Perdew (BP86)[51,52] exchange-correlation functional with a triple zeta with polarization (TZP) basis set was used for all molecules. To account for scalar relativistic effects, the Zero Order Regular Approximation (ZORA)[53–55] was utilized. Unrestricted calculations were employed to account for the unpaired electrons in the systems. A dispersion correction[56] was used for all computations. The clusters of interest had a neutral, cation, or dication charge.

III. RESULTS AND DISCUSSION

A. Bare silver clusters Ag_n^z (n = 2-6; z = 0, +1, +2)

Initially we consider the simplest cluster, Ag_2, in the neutral, cationic, and dicationic charge states. The isomers and relative energies of these systems are summarized in Table I, and the coordinates of optimized systems are provided in the supplementary material. The neutral and cationic structures optimized successfully. However, the dication undergoes Coulomb explosion and is not a stable structure. For the neutral system, the Ag-Ag distance is 2.61 Å, which increases to 2.84 Å for the cationic cluster.

The Ag_3^z (z = 0, +1, +2) clusters have two isomers: linear and triangular (Figure 1). As shown in Table I, the linear structure is the most stable form of the neutral and dication systems. The triangular shape is more favorable for the cation. For the neutral system, Ag_3 does not form an equilateral triangle; two bond lengths are calculated to be 3.04 Å while the third bond length is only 2.64 Å. However, for the cationic system, all three bond lengths are calculated to be 2.76-2.77 Å. For the dicationic system, the linear isomer is slightly (0.10 eV) lower in energy than the triangle; however, both systems have long Ag-Ag bond lengths of 3.64 Å and 3.37 Å, respectively.

Five structures are possible for the Ag_4^z (z = 0, +1, +2) systems: diamond, Y-shape, a related bent Y shape, linear, and tetrahedron. The lowest energy structures for each charge state are shown in Figure 1. The diamond shape is favored in both the neutral and cationic forms with both Y shapes only slightly higher in energy for both systems (Table I). The linear structure is 0.45 eV higher in energy than the diamond structure for the neutral system, and the tetrahedron is not stable for this charge state. The tetrahedron is the lowest energy structure for the dicationic system; this occurs because the system now only has two delocalized electrons within the core of the nanostructure, which is a magic number for highly symmetric isotropic systems such as the tetrahedron. Addition of one electron (i.e., the singly charged cationic structure) distorts the perfect tetrahedron and elongates two of the bonds; addition of two electrons to reach the neutral structure does not form a stable cluster.

TABLE I. Isomer shapes and relative energies (eV) for neutral, cationic, and dicationic pure silver clusters Ag_n at the BP86-D/TZP level of theory. Energies are relative to the lowest energy (bolded) structure. Dashed cells (—) denote that this structure was not stable for the given charge state.

n	Isomer	Neutral	Cation	Dication
2	Linear	**0.00**	**0.00**	—
3	Linear	**0.00**	1.14	**0.00**
3	Triangle	0.06	**0.00**	0.10
4	Diamond	**0.00**	**0.00**	—
4	Y shape	0.10	0.20	—
4	Bent Y	0.10	0.20	0.73
4	Linear	0.45	—	1.42
4	Tetrahedron	—	0.11	**0.00**
5	Trapezoid	**0.00**	0.04	0.18
5	House	0.11	0.40	—
5	Bowtie	0.38	0.02	0.29
5	Bipyramid	0.45	—	0.05
5	Mallet	0.59	0.60	0.31
5	A shape	0.73	—	—
5	Y shape	0.91	0.87	—
5	Linear	1.15	1.78	—
5	3D bowtie	—	**0.00**	0.25
5	Tetrahedron plus triangle	—	0.08	**0.00**
5	Antenna	—	—	0.06
6	Triangle	**0.00**	—	—
6	3D pentagon	0.20	—	—
6	3D bowtie	0.80	0.08	**0.00**
6	Bowtie	1.57	0.70	—
6	Butterfly	—	**0.00**	—
6	Diamond with bridge	—	0.05	—
6	Bipyramid plus triangle	—	0.08	—
6	3D trapezoid	—	0.13	0.06
6	Chevron	—	0.14	—
6	3D zigzag	—	0.54	—
6	2D zigzag	—	0.56	—
6	3D antenna	—	—	0.04

It should be noted that the dicationic system has a three-dimensional lowest energy structure. The 2D-3D crossover occurs at different numbers of silver atoms depending on the charge state. This also suggests that highly charged silver clusters are likely to be more compact than their neutral counterparts.

There are many possible isomers for the $n = 5$ systems. The increased number of atoms allows for a greater number of possible structures. The lowest energy structures for each charge state are shown in Figure 1 and coordinates for all observed structures and their energies are given in the supplementary material. The 2-dimensional trapezoid (Figure 1) is unique to the neutral system as the lowest-energy isomer. The lowest energy isomer for the neutral system is planar in agreement with previous work that suggested that the 2D-3D transition for the neutral Ag cluster does not occur until $Ag_{6\text{-}7}$.[57] The linear structures are no longer contenders for the lowest energy isomer as they are more than 1.0 eV less stable than the most favorable isomers (Table I). The +1 cationic system now exhibits a three-dimensional lowest-energy structure denoted 3D bowtie. This suggests the 2D-3D transition for the singly cationic geometries occurs at approximately $n = 5$, which is earlier than the crossover for the neutral system. The dication system also favors a 3D structure, as expected since we find that the 2D-3D transition for Ag_n^{2+} occurs at $n = 4$.

The $n = 6$ arrangement allows for ten different observed isomers. The most stable structures can be found in Figure 1. The linear structure is no longer observed at this level of theory. The neutral

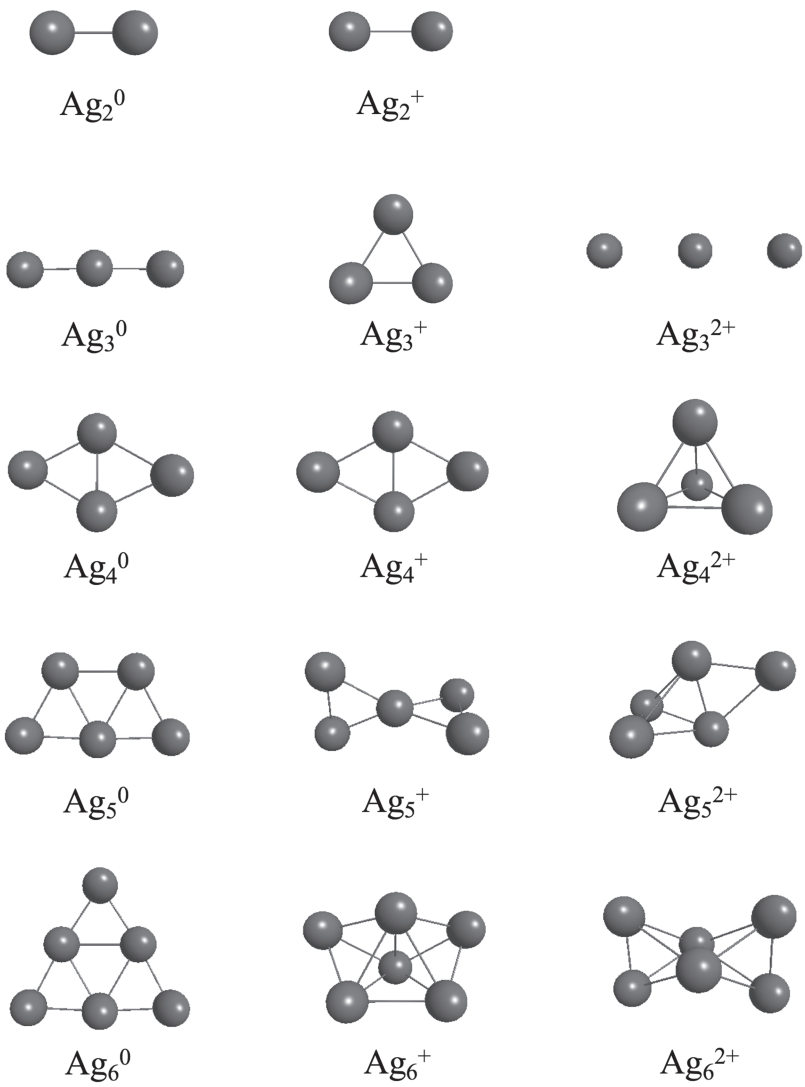

FIG. 1. Lowest energy structures for Ag_n^z (n = 2-6, z = 0-2) at the BP86-D level of theory.

system stays planar with a triangular shape. The lowest energy structure for the +1 system is a 3D butterfly structure. This is consistent with the 2D-3D transition for the cationic system occurring at Ag_5^+. Similarly, the lowest energy structure for the +2 system is three-dimensional, with a 3D bowtie structure. Thus, the structures of the neutral, singly, and doubly charged systems vary substantially, so it may be expected that silver clusters within complicated systems such as DNA-silver complexes will also have structures that depend on their exact charge state.

In comparison, Itoh *et al.* performed a study of neutral sodium, copper, and silver clusters (Ag_n, n = 2-75).[57] Their results for $Ag_{3\text{-}6}$ are comparable to those described above with one disparity. Their study suggests that the triangular Ag_3 is the lowest energy isomer by 0.028 eV whereas we calculate the linear isomer to be more stable by ~0.06 eV. This anomaly can be explained by their usage of the Perdew Wang functional (PW91) with a plane wave basis set and our procedure of Becke Perdew (BP86) with dispersion corrections (BP86-D) with a triple-zeta atom-centered basis set. In an analogous gold nanocluster study, Walker *et al.* looked at small gold clusters (Au_n, n = 2-9) in the neutral and singly charged cationic states.[58] Their results are similar to our results on silver clusters. They concluded that their lowest energy structures were the triangle for Au_3, trapezoid (called diamond in this work) for Au_4, X (bowtie) for Au_5, W (trapezoid) for Au_5^+, and triangle for Au_6.[58]

B. Guanine-silver complexes

We next investigated silver-guanine complexes. To avoid interactions that cannot occur in DNA-silver complexes, we capped nitrogen atom 9 with a methyl group rather than a hydrogen atom. We identified three positions where silver might interact with guanine without considering possible deprotonation of guanine. The first position (A in Figure 2) is on nitrogen 3 in the para location relative to carbon 6 in the C=O bond. The second possible binding position is located at nitrogen 7 (B in Figure 2). It is important to note here the proximity of the silver atoms to the oxygen atom in the carbonyl group. We will discuss this possible interaction later. The final location (C in Figure 2) involves the silver clusters interacting with the pi system above the primary plane of guanine. We employ the BP86-D approach to account for these dispersion interactions. This position does not have specific interactions with individual atoms in guanine.

We considered the interactions of the neutral, cation and dication isomers from Section III A with guanine at these three positions. Table II summarizes the lowest energy structures and relative energies for different positions on guanine. The lowest energy structure for each Ag_n^z-guanine system (n=3-6, z=0-2) is shown in Figure 3. Multiple silver cluster isomers were studied. For the neutral system, position A is the most favored position for cluster sizes 2 and 4. For neutral Ag_3, Ag_5, and Ag_6, the most favored position is C. Previous work for neutral silver-guanine interactions without dispersion

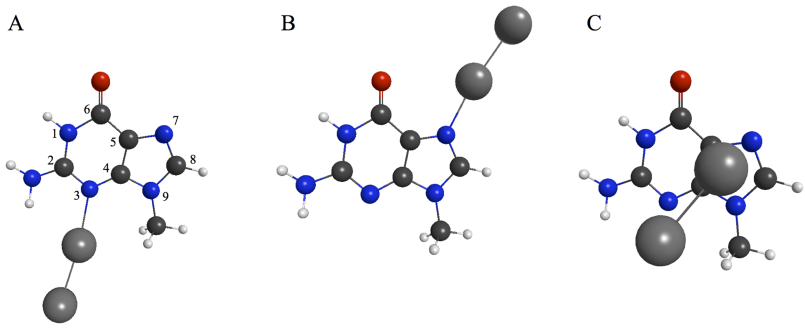

FIG. 2. Neutral Ag_2-guanine structures. The structures shown represent the three positions (A, B, and C) where the silver clusters can bind to guanine. The silver clusters in position C lie above the plane of guanine. Color key: Oxygen (red), nitrogen (blue), carbon (black), hydrogen (white), and silver (gray).

TABLE II. Relative energies (eV) for Ag_n^z-guanine systems. The isomers reported here are the calculated lowest energy structures from the bare Ag_n systems. The values in bold represent the guanine interaction position with the lowest energy. All energies are displayed relative to those values. Dashed cells (—) denote that this structure was not stable for the given charge state.

n	Charge (z)	Isomer	Position A	Position B	Position C
2	0	Linear	0.00	0.06	0.27
2	1+	Linear	0.85	0.00	—
3	0	Linear	0.01	0.01	0.00
3	1+	Triangle	1.07	0.00	—
3	2+	Linear	—	—	—
3	2+	Triangle	1.08	0.00	—
4	0	Diamond	0.00	0.39	0.21
4	1+	Diamond	1.17	0.00	—
4	2+	Tetrahedron	1.84	0.00	—
5	0	Trapezoid	0.29	0.34	0.00
5	1+	3D bowtie	1.23	0.00	0.43
5	2+	Tetrahedron plus triangle	1.79	0.00	—
6	0	Triangle	0.37	0.42	0.00
6	1+	Butterfly/3D pentagon	0.83	0.00	0.14
6	2+	3D bowtie	—	0.00	—

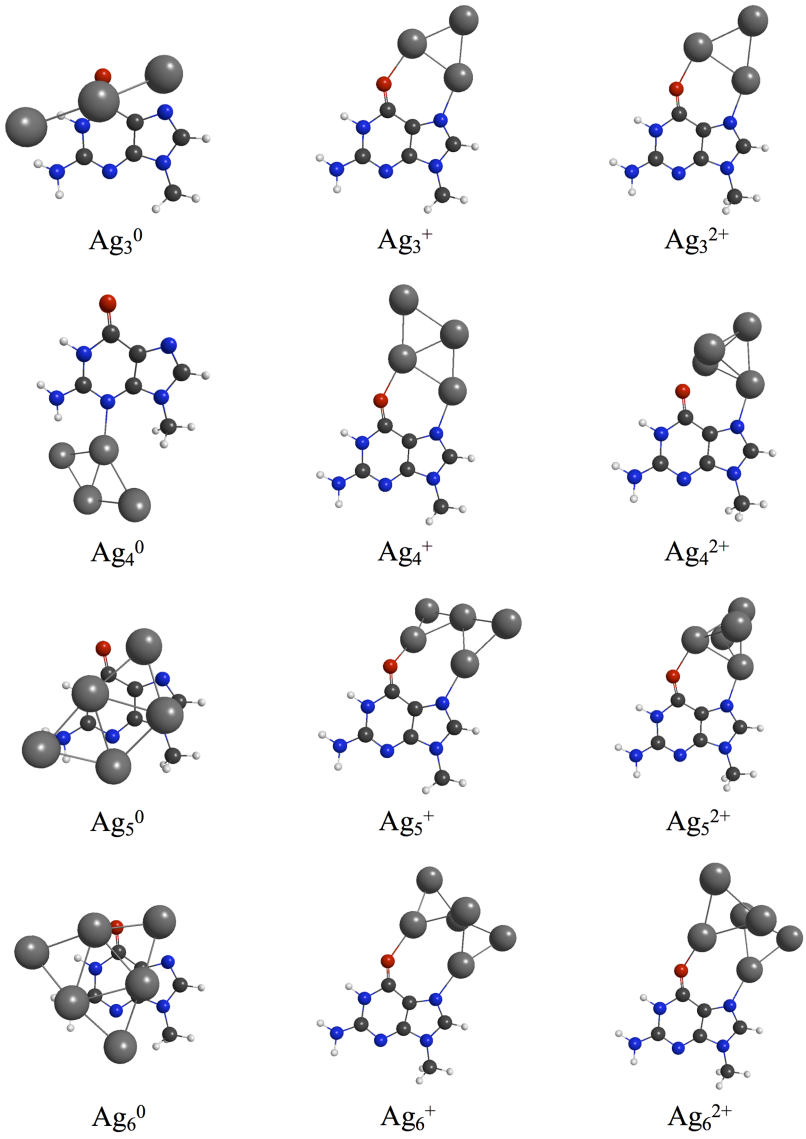

FIG. 3. Lowest energy structures for Ag_n^z-guanine systems (n=3-6, z=0-2).

corrections did not predict interactions with the pi system.[40] In contrast, all of the cationic systems interact preferentially at position B. This position was also observed in previous work on individual silver cations interacting with guanine.[41] Since the silver-DNA complexes are experimentally known to be positively charged,[33,59,60] this suggests that the most favorable interaction for these clusters with guanine bases may occur through nitrogen 7 and the neighboring carbonyl group. For the cation and dication systems, nearly all silver clusters in position B appeared to interact with the oxygen atom as well as the nitrogen. A delocalized 1+ or 2+ charge on the silver nanocluster most likely associates with the lone pairs on the oxygen to promote this interaction. In contrast, the neutral silver systems do not interact with the oxygen lone pairs. It should be noted that the work presented here focuses on single DNA bases in the gas phase, and different interactions may be preferred for base pairs and for bases in solution.[61]

In general, the shape of the silver cluster remains very similar to the shape of the isolated silver cluster. Aside from a few exceptions discussed in this paragraph, the shape of the silver cluster does not change upon binding with guanine. This suggests that developing an understanding of the shapes of charged metal clusters can provide a very good indication of the shape of the metal cluster when

TABLE III. Binding energies (eV) for the lowest energy complexes of Ag_n^z clusters with guanine. The sites where the cluster binds with guanine are denoted (A), (B), or (C).

Complex	Binding energy (eV)
Ag_2^0-guanine (A)	0.80
Ag_2^+-guanine (B)	2.61
Ag_3^0-guanine (C)	0.73
Ag_3^+-guanine (B)	2.50
Ag_3^{2+}-guanine (B)	5.29[a]
Ag_4^0-guanine (A)	1.20
Ag_4^+-guanine (B)	2.38
Ag_4^{2+}-guanine (B)	4.35
Ag_5^0-guanine (C)	1.05
Ag_5^+-guanine (B)	2.48[b]
Ag_5^{2+}-guanine (B)	4.21[c]
Ag_6^0-guanine (C)	1.13
Ag_6^+-guanine (B)	2.25
Ag_6^{2+}-guanine (B)	3.93

[a]Binding energy calculated using triangle structure for Ag_3^{2+}.
[b]Binding energy calculated using 3D bowtie structure for Ag_5^+.
[c]Binding energy calculated using bipyramid structure for Ag_5^{2+}.

it interacts with DNA. When Ag_3^{2+} binds with guanine, the preferred structure in the complex is the triangle shape rather than the linear orientation. This allows two silver atoms to interact with nitrogen 7 and the neighboring carbonyl group, which is expected to increase the magnitude of its binding energy. This system has a binding energy of 5.29 eV relative to isolated guanine and the triangular Ag_3^{2+} structure, which is the largest binding energy observed in this work (Table III). The Ag_5^+-guanine complex has a trapezoid-like silver cluster rather than the initial 3D bowtie structure. It should be noted that these isomers are very close in energy (0.04 eV) for the bare silver systems, so it is not surprising that the presence of DNA provides enough of a perturbation to affect the observed isomer. The silver cluster in the complex can be described as a slightly nonplanar trapezoid or as a planarized 3D bowtie. The last system in which a different isomer was observed in the complex than in the isolated silver cluster is the Ag_5^{2+}-guanine system. In this complex, the bipyramid structure is observed. Again, this isomer was only slightly (0.05 eV) higher in energy than the "tetrahedron plus triangle" structure that was found to be the lowest energy for the isolated system. Overall, the metal cluster in the silver-DNA complex is found to either be the lowest energy isomer or a very close-lying isomer.

The binding energies of these systems are shown in Table III. Binding energies are calculated according to the standard formula as $Binding\ Energy = E(Ag_z^n) + E(\text{guanine}) - E(Ag_z^n\text{-guanine complex})$. Thus, positive binding energies correspond to favorable binding interactions. Binding energies for the neutral systems are the smallest. These range from 0.73 to 1.20 eV at the BP86-D/TZP level of theory. It should be noted that binding energies at this level of theory may be overestimated, although binding energies with the standard BP86 functional are typically underestimated. Binding energies are significantly larger for singly charged systems, with calculated energies of 2.25-2.61 eV. The dicationic systems exhibit even larger binding energies of 3.93-5.29 eV.

IV. CONCLUSIONS

In this work, density functional theory calculations at the BP86-D/TZP level of theory were performed to predict the structures of bare silver clusters Ag_n^z (n = 2-6; z = 0, +1, +2) and their complexes with guanine. All neutral silver clusters in this work are predicted to be planar, whereas the cationic systems undergo a 2D-3D transition between Ag_4 and Ag_5, and the dicationic systems experience a 2D-3D transition between Ag_3 and Ag_4. In general, the clusters with a higher charge are more compact. Many of the structural trends are preserved upon binding to a guanine base. In

general, the isomers observed for silver-DNA complexes in this work have silver cluster structures similar to those of the most stable or energetically low-lying isomers of isolated silver clusters.

Although neutral silver clusters bind with nitrogen 3 or with the pi system of the base, positively charged clusters preferentially interact with nitrogen 7 and the neighboring carbonyl group. Thus, the cationic silver-DNA clusters present experimentally may interact with nitrogen 7 and the carbonyl group of guanine bases. Additional work on the interactions of cationic silver clusters with other DNA bases, base pairs, and in solution will be needed to fully understand the structures present experimentally.

SUPPLEMENTARY MATERIAL

See supplementary material for coordinates of bare silver clusters and silver-guanine complexes discussed in this work.

ACKNOWLEDGMENTS

This material is based on work supported by the National Science Foundation under Grant No. CHE-1507909. C.M.A. is grateful to the Camille and Henry Dreyfus Foundation for a Camille Dreyfus Teacher-Scholar Award (2011–2016).

[1] M. Harb, F. Rabilloud, D. Simon, A. Rydlo, S. Lecoultre, F. Conus, V. Rodrigues, and C. Félix, J. Chem. Phys. **129**, 194108 (2008).
[2] M. L. Tiago, J. C. Idrobo, S. Öğüt, J. Jellinek, and J. R. Chelikowsky, Phys. Rev. B **79**(15), 155419 (2009).
[3] B. Sengupta, C. M. Ritchie, J. G. Buckman, K. R. Johnsen, P. M. Goodwin, and J. T. Petty, J. Phys. Chem. C **112**(48), 18776–18782 (2008).
[4] A. Latorre and Á. Somoza, ChemBioChem **13**(7), 951–958 (2012).
[5] Z. Yuan, Y.-C. Chen, H.-W. Li, and H.-T. Chang, Chem. Commun. **50**(69), 9800–9815 (2014).
[6] S. Choi, R. M. Dickson, and J. Yu, Chem. Soc. Rev. **41**(5), 1867–1891 (2012).
[7] J. Liu, Trends Anal. Chem. **58**, 99–111 (2014).
[8] J. T. Petty, S. P. Story, J.-C. Hsiang, and R. M. Dickson, J. Phys. Chem. Lett. **4**(7), 1148–1155 (2013).
[9] E. Gwinn, D. Schultz, S. Copp, and S. Swasey, Nanomaterials **5**(1), 180 (2015).
[10] B. Han and E. Wang, Anal. Bioanal. Chem. **402**(1), 129–138 (2012).
[11] Y.-C. Shiang, C.-C. Huang, W.-Y. Chen, P.-C. Chen, and H.-T. Chang, J. Mater. Chem. **22**(26), 12972–12982 (2012).
[12] J. M. Obliosca, C. Liu, and H.-C. Yeh, Nanoscale **5**(18), 8443–8461 (2013).
[13] S. Y. New, S. T. Lee, and X. D. Su, Nanoscale **8**(41), 17729–17746 (2016).
[14] L. Zhang and E. Wang, Nano Today **9**(1), 132–157 (2014).
[15] I. Diez and R. H. A. Ras, Nanoscale **3**(5), 1963–1970 (2011).
[16] H. Xu and K. S. Suslick, Adv. Mater. **22**(10), 1078–1082 (2010).
[17] T. Zhou, Y. Huang, W. Li, Z. Cai, F. Luo, C. J. Yang, and X. Chen, Nanoscale **4**(17), 5312–5315 (2012).
[18] J. T. Petty, J. Zheng, N. V. Hud, and R. M. Dickson, J. Am. Chem. Soc. **126**(16), 5207–5212 (2004).
[19] C. I. Richards, S. Choi, J.-C. Hsiang, Y. Antoku, T. Vosch, A. Bongiorno, Y.-L. Tzeng, and R. M. Dickson, J. Am. Chem. Soc. **130**(15), 5038–5039 (2008).
[20] J. Sharma, R. C. Rocha, M. L. Phipps, H.-C. Yeh, K. A. Balatsky, D. M. Vu, A. P. Shreve, J. H. Werner, and J. S. Martinez, Nanoscale **4**(14), 4107–4110 (2012).
[21] J. T. Petty, D. A. Nicholson, O. O. Sergev, and S. K. Graham, Anal. Chem. **86**(18), 9220–9228 (2014).
[22] J. T. Petty, C. Fan, S. P. Story, B. Sengupta, A. St. John Iyer, Z. Prudowsky, and R. M. Dickson, J. Phys. Chem. Lett. **1**(17), 2524–2529 (2010).
[23] J. Obliosca, C. Liu, R. Batson, M. Babin, J. Werner, and H.-C. Yeh, Biosensors **3**(2), 185 (2013).
[24] C. Ma, C. Lin, Y. Wang, and X. Chen, Trends Anal. Chem. **77**, 226–241 (2016).
[25] Y. Tao, M. Li, J. Ren, and X. Qu, Chem. Soc. Rev. **44**(23), 8636–8663 (2015).
[26] Y. Tao, Z. Li, E. Ju, J. Ren, and X. Qu, Chem. Commun. **49**(61), 6918–6920 (2013).
[27] P. R. O'Neill, K. Young, D. Schiffels, and D. K. Fygenson, Nano Lett. **12**(11), 5464–5469 (2012).
[28] Z. Huang, F. Pu, Y. Lin, J. Ren, and X. Qu, Chem. Commun. **47**(12), 3487–3489 (2011).
[29] T. Molotsky, T. Tamarin, A. B. Moshe, G. Markovich, and A. B. Kotlyar, J. Phys. Chem. C **114**(38), 15951–15954 (2010).
[30] C. M. Ritchie, K. R. Johnsen, J. R. Kiser, Y. Antoku, R. M. Dickson, and J. T. Petty, J. Phys. Chem. C **111**(1), 175–181 (2007).
[31] G. Shemer, O. Krichevski, G. Markovich, T. Molotsky, I. Lubitz, and A. B. Kotlyar, J. Am. Chem. Soc. **128**(34), 11006–11007 (2006).
[32] J. Wu, Y. Fu, Z. He, Y. Han, L. Zheng, J. Zhang, and W. Li, J. Phys. Chem. B **116**(5), 1655–1665 (2012).
[33] D. Schultz, K. Gardner, S. S. R. Oemrawsingh, N. Markešević, K. Olsson, M. Debord, D. Bouwmeester, and E. Gwinn, Adv. Mater. **25**(20), 2797–2803 (2013).
[34] S. M. Copp, P. Bogdanov, M. Debord, A. Singh, and E. Gwinn, Adv. Mater. **26**(33), 5839–5845 (2014).
[35] E. G. Gwinn, P. O'Neill, A. J. Guerrero, D. Bouwmeester, and D. K. Fygenson, Adv. Mater. **20**(2), 279–283 (2008).

[36] S. M. Copp, D. Schultz, S. Swasey, J. Pavlovich, M. Debord, A. Chiu, K. Olsson, and E. Gwinn, J. Phys. Chem. Lett. **5**(6), 959–963 (2014).
[37] J. M. Obliosca, M. C. Babin, C. Liu, Y.-L. Liu, Y.-A. Chen, R. A. Batson, M. Ganguly, J. T. Petty, and H.-C. Yeh, ACS Nano **8**(10), 10150–10160 (2014).
[38] H.-C. Yeh, J. Sharma, J. J. Han, J. S. Martinez, and J. H. Werner, Nano Lett. **10**(8), 3106–3110 (2010).
[39] H. C. Yeh, J. Sharma, J. J. Han, J. S. Martinez, and J. H. Werner, IEEE Nanotechnol. Mag. **5**(2), 28–33 (2011).
[40] V. Soto-Verdugo, H. Metiu, and E. Gwinn, J. Chem. Phys. **132**(19), 195102 (2010).
[41] L. A. Espinosa Leal and O. Lopez-Acevedo, Nanotechnol. Rev. **4**(2), 173–191 (2015).
[42] S. M. Swasey, L. Espinosa Leal, O. Lopez-Acevedo, J. Pavlovich, and E. G. Gwinn, Sci. Rep. **5**, 10163 (2014).
[43] R. R. Ramazanov and A. I. Kononov, J. Phys. Chem. C **117**(36), 18681–18687 (2013).
[44] R. R. Ramazanov, T. S. Sych, Z. V. Reveguk, D. A. Maksimov, A. A. Vdovichev, and A. I. Kononov, J. Phys. Chem. Lett. **7**(18), 3560–3566 (2016).
[45] S. M. Swasey, N. Karimova, C. M. Aikens, D. E. Schultz, A. J. Simon, and E. G. Gwinn, ACS Nano **8**(7), 6883–6892 (2014).
[46] P. K. Samanta, A. K. Manna, and S. K. Pati, Chem. - Asian J. **7**(11), 2718–2728 (2012).
[47] R. Longuinhos, A. Lúcio, H. Chacham, and S. Alexandre, Phys. Rev. E **93**(5), 052413 (2016).
[48] M. Berdakin, M. Taccone, K. J. Julian, G. Pino, and C. G. Sánchez, J. Phys. Chem. C **120**(42), 24409–24416 (2016).
[49] G. te Velde, F. M. Bickelhaupt, E. J. Baerends, C. Fonseca Guerra, S. J. A. van Gisbergen, J. G. Snijders, and T. Ziegler, J. Comput. Chem. **22**(9), 931–967 (2001).
[50] C. Fonseca Guerra, J. G. Snijders, G. te Velde, and E. J. Baerends, Theor. Chem. Acc. **99**(6), 391–403 (1998).
[51] A. D. Becke, Phys. Rev. A **38**(6), 3098–3100 (1988).
[52] J. P. Perdew, Phys. Rev. B **34**(10), 7406 (1986).
[53] E. van Lenthe, A. Ehlers, and E.-J. Baerends, J. Chem. Phys. **110**(18), 8943–8953 (1999).
[54] E. van Lenthe, E. J. Baerends, and J. G. Snijders, J. Chem. Phys. **101**(11), 9783–9792 (1994).
[55] E. v. Lenthe, E. J. Baerends, and J. G. Snijders, J. Chem. Phys. **99**(6), 4597–4610 (1993).
[56] S. Grimme, J. Comput. Chem. **27**(15), 1787–1799 (2006).
[57] M. Itoh, V. Kumar, T. Adschiri, and Y. Kawazoe, J. Chem. Phys. **131**(17), 174510 (2009).
[58] A. V. Walker, J. Chem. Phys. **122**(9), 094310–094312 (2005).
[59] J. T. Petty, O. O. Sergev, A. G. Kantor, I. J. Rankine, M. Ganguly, F. D. David, S. K. Wheeler, and J. F. Wheeler, Anal. Chem. **87**, 5302–5309 (2015).
[60] J. T. Petty, O. O. Sergev, M. Ganguly, I. J. Rankine, D. M. Chevrier, and P. Zhang, J. Am. Chem. Soc. **138**, 3469–3477 (2016).
[61] L. A. Espinosa Leal, A. Karpenko, S. Swasey, E. G. Gwinn, V. Rojas-Cervellera, C. Rovira, and O. Lopez-Acevedo, J. Phys. Chem. Lett. **6**, 4061–4066 (2015).